J|A|C|S COMMUNICATIONS

Published on Web 10/15/2010

3-D Carbon Nanotube Structures Used as High Performance Catalyst for Oxygen Reduction Reaction

Wei Xiong,[†,§] Feng Du,[‡] Yong Liu,[‡] Albert Perez, Jr.,[†] Michael Supp,[†] Terizhandur S. Ramakrishnan,[†] Liming Dai,[‡] and Li Jiang*[,†]

Schlumberger-Doll Research, 1 Hampshire Street, Cambridge, Massachusetts 02139, and Department of Chemical Engineering, Case Western Reserve University, 10900 Euclid Avenue, Cleveland, Ohio 44106

Received May 21, 2010; E-mail: ljiang@slb.com

Abstract: We report a high performance oxygen reduction reaction (ORR) catalyst based on vertically aligned, nitrogen-doped carbon nanotube (VA-NCNT) arrays. Characterization in conditions analogous to the operation of a polymer electrolyte membrane fuel cell show ORR taking place on the catalyst at a favorable reduction potential with a superior current density and greater rate constant.

In light of the increasingly dire challenges in the intertwined fronts of energy and climate change, the pursuit of environment friendly *"green"* energy sources becomes ever more pertinent. Among the most probable options to alternative energy sources is the fuel cell, in particular the polymer electrolyte fuel cell (PEMFC) that proffers instant power output with high energy conversion efficiency and high power density in the absence of any flame, combustion, noise, or vibration. In principle, the carbon neutral PEMFC consumes hydrogen as fuel that forms the foundation of the much debated hydrogen economy.

In addition to the economics, the most severe bottleneck that prevents the PEMFC from reaching its full technical potential lies in the undesirably low performance of—in particular the cathode—catalyst. At present, the oxygen reduction reaction (ORR) rate—as measured by the standard state (298 K, 1 atm) exchange current density—on the cathode catalyst, commonly in the form of platinum spheres in the 2 nm diameter domain, is 6 orders of magnitude slower than that of its anodic counterpart.[1] Entangled by the concurrence of a host of conflicting side reactions on common catalyst and electrode interfaces, it contributes to a significant overpotential that undermines the performance of the PEMFC in the form of a kinetic hurdle.

The anode reaction of hydrogen oxidation is relatively facile involving a single electron transfer process. While, in comparison, the cathode reaction of ORR is a far more complex four-electron transfer process involving a cascade of key elementary steps.[2−4] The origin of such a huge disparity in reaction rate is due to the kinetic sluggishness of the ORR at the cathode afflicted by the multiple-step nature of a given catalyst surface.

Extensive efforts are underway to enhance the catalytic performance of Pt based catalysts. For example, a family of catalysts using a Pt monolayer coated on non-noble metal substrates not only enhances the ORR catalytic efficiency but also considerably reduces the requirement of Pt to be used in the fuel cell.[5] Binary alloys of Pt in a general format Pt_3M (M = Ni, Co, Fe, Ti, V, Pd, Mo, W, Cu, Ru)[6−8] are promising as it is believed that the presence of the M species changes the electronic configuration of Pt, leading to a weaker interaction between the Pt surface and the unwanted PtOH intermediate. A recent report on Pt−Pd nanodendrites exhibited higher ORR activity particularly at certain crystallite facets.[9] Concerns regarding the global supply of platinum material as fuel cell catalysts prompted the exploration of other non-noble metal compounds, notably some cobalt−corrole,[10] cobalt−polypyrrole,[11] and iron−N_4[12] complexes. Additionally, the cost of Pt is also an issue of concern. For example, it was estimated that, on the basis of a recent peak price of Pt, in July, 2008, at over $2200/oz, the cost of Pt alone used in a 100-kW PEMFC engine (~0.8 g per kW) is substantially greater than the current cost of an entire internal combustion gasoline engine of equal power.[13]

Various forms of carbon are commonly used as electrode materials to support the metallic catalysts, a recent addition of which is the single atomic layer graphite, graphene.[14]

Most recently some of us reported an entirely metal-free catalyst system containing vertically aligned, nitrogen-doped carbon nanotubes (VA-NCNTs) for oxygen reduction reaction in an alkaline medium.[15] It was hypothesized that the catalytic function of VA-NCNTs originates from the disparity of the charge density distribution of carbon atoms around the dopant.

We investigated the use of nitrogen-doped carbon nanotube arrays as an oxygen reduction reaction (ORR) catalyst in a PEMFC-analogous acidic medium, showing a strong ORR signal at the favorably positive potential. The results unambiguously support a desirable catalyst material with a higher current density and greater ORR rate constant. The superior catalytic performance is manifested by the facile steady state electrochemical feature shown in the voltammograms that is in sharp contrast to those transient ones with conventional Pt-based catalysts.

The vertically aligned, nitrogen-doped carbon nanotube (VA-NCNT) arrays were manufactured in a protocol analogous to those in the literature.[16−20] In brief, on a cleaned silicon wafer coated with a 100 nm thick layer of silica, a mixture of Ar, H_2, and NH_3 gases of certain proportion were reacted at around 850 °C, in the presence of a catalyst pyrolyzing iron(II) phthalocyanine, for a period of 2 h. Shown in Figure 1 are two SEM images of different magnification of such a VA-NCNT sample, exhibiting highly ordered 3D array structures of individual NCNTs in an orientation perpendicular to the substrate and at a well-defined distance from the adjacent counterparts. These NCNTs as viewed from the cross section display a uniform length of 7.5 μm (left). The high resolution SEM on the right-hand side shows a uniform width of individual NCNTs as ~50 nm. In the current experimental setup, the height and diameter of NCNTs, as well as the density of NCNT coverage on the substrate, are tunable by adjusting the parameters in the synthetic protocol. The then prepared VA-NCNT was removed,

[†] Schlumberger-Doll Research.
[‡] Case Western Reserve University.
[§] On leave from University of Dayton.

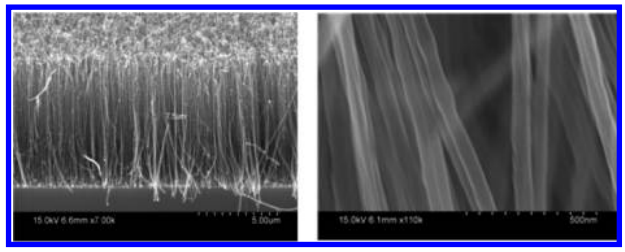

Figure 1. SEM images of vertically aligned nitrogen doped carbon nanotubes.

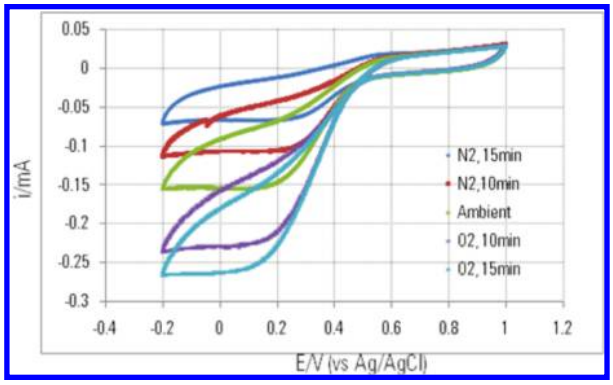

Figure 2. Steady state voltammograms showing oxygen reduction reaction taking place on VA-NCNT at various oxygen partial pressures. Potential scan rate 5 mV cm^{-1} with the third scans shown.

via a benign wet chemistry procedure, from the silica/silicon substrate and transferred onto a platinum mesh, or a planar glassy carbon electrode surface, for subsequent electrochemical tests (see Supporting Information).

The identification of the oxygen reduction signal on the VA-NCNTs was achieved by varying the concentration of molecular oxygen dissolved in the solution, as shown in Figure 2. In an aqueous solution mimicing the chemical environment of a PEMFC, a discrete reduction current is proportional to the concentration of dioxygen. The voltammograms exhibited virtually steady state features, including the reduction current plateau and literally zero reoxidation current. In combination, these features indicate a rapid electron transfer process of ORR. It is worth noting that the steady state features remained across the potential scan rate range from 1 to 150 mV s^{-1}. In addition, the strict linear relationship between the reduction current over the square root of the potential scan rate corroborates that the reductive species is dissolved in the bulk of the solution (see Supporting Information for more details).

The rate of the electron transfer reaction at the VA-NCNT surface was measured by applying the electrode configuration to a pure single electron transfer reaction as exerted by the well characterized redox couple, ferro/ferricyanide, $Fe(CN)_6^{4-}/Fe(CN)_6^{3-}$, in an aqueous solution using cyclic voltammetry. It was determined using the Randles−Sevcik equation that the effective electrochemical surface area of a particular VA-NCNT electrode is 0.29 cm^2 (see Supporting Information). With a total geometric area of the same electrode estimated as 69.8 cm^2 (see the Supporting Information), this leads to a ratio of 0.42% associated with the present packaging protocol, through which the vast majority of the surface is electrochemically inaccessible as a result of coverage by polystyrene that is critical to maintaining the 3D structural integrity of VA-NCNTs.

Based on the above calculation, it can be concluded that the observed current density is 2.62×10^{-3} A cm^{-2}, which closely resembles the kinetic limiting current density, in the absence of any perturbation of the solution. Therefore the ORR rate constant can be estimated as 5.38×10^{-3} cm s^{-1}. This ORR rate constant compares favorably with those obtained on Pt-based common catalysts.

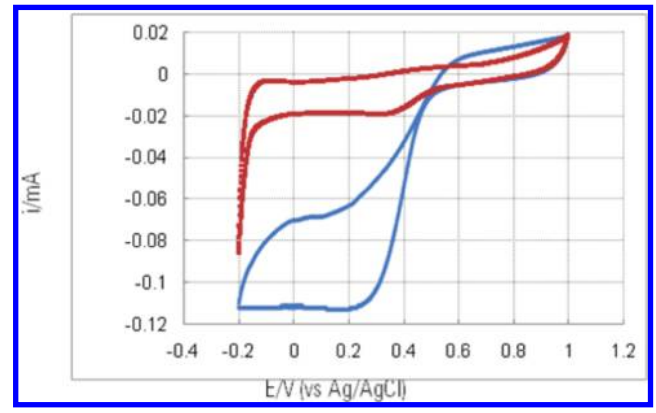

Figure 3. ORR electrocatalytic profile of a Pt black on glassy carbon electrode (red) and a VA-NCNT on Pt mesh (blue) electrode immersed in an air saturated solution containing H_2SO_4 (pH = 3). Potential scan rate: 5 mV s^{-1} with the third scans shown.

The steady state characteristics of the ORR as shown in Figure 2 are in contrast to the transient voltammetric feature of the $Fe(CN)_6^{4-}/Fe(CN)_6^{3-}$ couple (Figure S4). This further corroborates the fact that the catalytic ORR only takes place at the N-bearing sites, the low abundance of which makes individual sites functioning as sparsely distributed arrays of electrodes whose diffusion layers do not overlap.

A critical comparison of the VA-NCNT's catalytic performance is made in Figure 3 against the commonly used Pt-black catalyst, which is essentially Pt particles of 2.2 nm in diameter dispersed onto a carbon black support. About 90 μg of Pt-black generated an ~20 μA peak-shaped transient ORR current. In contrast, a sum of 50 μg (electrochemically accessible) of VA-NCNT yielded an ~120 μA steady state ORR current. In addition to the significantly greater current output, the VA-NCNT also results in an ~47 mV anodic shift in oxygen reduction potential.

It is remarkable that the current density can be translated into the volumetric unit of active VA-NCNT material as 2108.3 A cm^{-3}(see Supporting Information). This value represents a staggering 62% higher performance than the entrance benchmark commonly accepted for the ORR catalysts.[21] This is critical in controlling the performance of the catalysts under fuel cell operation conditions.

In summary, we have demonstrated the application of a completely metal-free catalyst system of ORR using VA-NCNTs, which exhibits a number of desirable aspects in comparison with the more conventional materials. Currently, effort is underway to evaluate the performance of the new catalyst being utilized in membrane electrode assembly and tested under fuel cell operation conditions.

Acknowledgment. W.X. wishes to thank Schlumberger for support through an internship.

Supporting Information Available: Details of VA-NCNT electrode preparation procedure, general electrochemistry parameters, calculation of effective electrochemical surface area, current density, and rate constant of catalytic reduction of oxygen. This material is available free of charge via the Internet at http://pubs.acs.org.

References

(1) O'Hayre, R. P. Cha, S.-W. Colella, W. Prinz, F. B. *Fuel cell fundamentals*; John Wiley & Sons: New York, 2006; pp 83−84.
(2) Appleby, A. J. *J. Electroanal. Chem.* **1993**, *357*, 117–179.
(3) Adzic, R. *Recent advances in the kinetics of oxygen reduction in electrocatalysis*; Lipkowski, J., Ross, P. N., Eds.; Wiley-VCH: New York, 1998; pp 197−242.
(4) Schmidt, T. J. Markovic, N. M. *Encyclopedia of surface and colloid science*; Taylor & Francis: 2006; pp 2032−2047.
(5) Zhang, J.; Lima, F. H. B.; Shao, M. H.; Kasaki, K.; Wang, J. X.; Hanson, J.; Adzic, R. R. *J. Phys. Chem. B* **2005**, *109*, 22701–22704.
(6) Zhang, J.; Sasaki, K.; Sutter, E.; Adzic, R. R. *Science* **2007**, *315*, 220–222.
(7) Stamenkovic, V. R.; Flower, B.; Mun, B. S.; Wang, G.; Ross, P. N.; Lucas, C. A.; Markovic, N. M. *Science* **2007**, *315*, 493–497.
(8) Stamenkovic, V. R.; Mun, B. S.; Mayrhofer, K. J. J.; Ross, P. N.; Markovic, N. M.; Greeley, J.; Nørskov, J. N. *Angew. Chem., Int. Ed.* **2006**, *45*, 2897–2901.
(9) Lim, B.; Jiang, M.; Camargo, P. H. C.; Cho, E. C.; Tao, J.; Lu, X.; Zhu, Y.; Xia, Y. *Science* **2009**, *324*, 1302–1305.
(10) Kadish, K. M.; Frémond, L.; Ou, Z.; Shao, J.; Shi, C.; Anson, F. C.; Burdet, F.; Gros, C. P.; Barbe, J. M.; Guilard, R. *J. Am. Chem. Soc.* **2005**, *127*, 5625–5631.
(11) Bashyam, R.; Zelenay, P. *Nature* **2006**, *443*, 63–66.
(12) Lefèvre, M.; Proietti, E.; Jaouen, F.; Dodelet, J. P. *Science* **2009**, *324*, 71–74.
(13) http://www.kitco.com/charts/liveplatinum.html (retrieved July 30, 2009).
(14) Kou, R.; Shao, Y.; Wang, D.; Engelhard, M. H.; Hwak, J. H.; Wang, J.; Viswanathan, V. V.; Wang, C.; Lin, Y.; Wang, Y.; Aksay, I. A.; Liu, J. *Electrochem. Commun.* **2009**, *5*, 954–957.
(15) Gong, K.; Du, F.; Durstock, M.; Dai, L. *Science* **2009**, *323*, 760–764.
(16) Terrones, M.; Redlich, P.; Gilbert, N.; Trasobares, S.; Hsu, W. K.; Terrones, H.; Zhu, Y. -Q.; Hare, J. P.; Reeves, C. L.; Cheetham, A. K.; Ruhle, M.; Kroto, H. W.; Walton, D. R. M. *Adv. Mater.* **1999**, *11*, 655–958.
(17) Bajpai, V.; Dai, L.; Ohashi, T. *J. Am. Chem. Soc.* **2004**, *126*, 5070–5071.
(18) He, M.; Zhou, S.; Zhang, J.; Liu, Z.; Robinson, C. *J. Phys. Chem. B* **2005**, *109*, 9275–9279.
(19) Allen, B. L.; Kichambare, P. D.; Star, A. *ACS Nano* **2008**, *2*, 1914–1920.
(20) Yang, J.; Liu, D. J.; Kariuki, N. N.; Chen, L. X. *Chem. Commun.* **2008**, *329*, 329–331.
(21) Gasteiger, H. A.; Kocha, S. K.; Sompalli, B.; Wagner, F. T. *Appl. Catal., B* **2005**, *56*, 9–35.

JA104425H